# Soliton-emitting AlGaAs waveguide

**Patrick Dumais and Alain Villeneuve**

*Pavillon Vachon, Université Laval, Cité Universitaire, Québec, Canada G1K 7P4*
*pdumais@phy.ulaval.ca*

**Amr Saher-Helmy and J. Stewart Aitchison**

*Department of Electronics and Electrical Engineering, University of Glasgow, Glasgow, Scotland, G12 8QQ, United Kingdom*

**Abstract:** Simulations of soliton emission and propagation in a linear AlGaAs waveguide with one nonlinear cladding are presented. The device, which has realistic parameters, operates below half the bandgap and emits light into the cladding for a given input power. The use of selective disordering of the MQW guiding layer to realize the linear/nonlinear sections is discussed.

**OCIS codes:** (190.4390) Nonlinear optics, integrated optics; (190.4360) Nonlinear optics, devices

**References**

1. G. I. Stegeman, C. T. Seaton, J. Chilwell and D. Smith., "Nonlinear waves guided by thin films," Appl. Phys. Lett. **44**, 830-832 (1984).
2. C. T. Seaton, J. D. Valera, R. L. Shoemaker, G. I. Stegeman, J. T. Chilwell and S. D. Smith, "Calculations of nonlinear TE waves guided by Thin Dielectric Films Bounded by Nonlinear Media," IEEE J. Quantum Electron. **QE-21**, 774-783 (1985).
3. J. V. Moloney, J. Ariyasu, C. T. Seaton and G. I. Stegeman, "Stability of nonlinear stationary waves guided by a thin film bounded by nonlinear media," Appl. Phys. Lett. **48**, 826-828 (1986).
4. D. R. Heatley, E. M. Wright, and G. I. Stegeman, "Soliton coupler," Appl. Phys. Lett. **53**, 172-174 (1988).
5. C. J. Hamilton, J. H. Marsh, D. C. Hutchings, J. S. Aitchison, G. T. Kennedy and W. Sibbett, "Localized Kerr-type nonlinearities in GaAs/AlGaAs multiple quantum well structures at 1.55 µm," Appl. Phys. Lett. **68**, 3078-3080 (1996).
6. B. S. Ooi, K. McIlvaney, M. W. Street, A. Saher Helmy, S. G. Ayling, A. C. Bryce, J. H. Marsh, and J. S. Roberts, " Selective quantum-well intermixing on GaAs-AlGaAs structures using impurity-free vacancy diffusion," IEEE J. Quantum Electron. **QE-33**, 1784-1793 (1997).
7. R. J. Deri and M. A. Emanuel, "Consistent formula for the refractive index of Al(1-x)Ga(x)As below the band edge," J. Appl. Phys., "Optical dispersion relations for GaP, GaAs, GaSb, InP, InAs, InSb, AlxGa1xAs, and In1xGaxAsyP1y", **77**, 4667 (1995).
8. S. Adachi, "Optical dispersion relations for GaP, GaAs, GaSb, InP, InAs, InSb, $Al_xGa_{1-x}As$, and $In_{1-x}Ga_xAs_yP_{1-y}$ ,"J. Appl. Phys. **66**, 6030 (1989).
9. M. Sheik-Bahae, D. C. Hutchings, D. J. Hagan and E. W. Van Stryland, "Dispersion of bound electronic nonlinear refraction in solids," IEEE J. Quantum Electron., **27**, 1296-1309 (1991).
10. C. C. Yang, A. Villeneuve, G. I. Stegeman, Cheng-Hui Lin and Hao-Hsiung Lin, "Anisotropic Two-Photon Transitions in GaAs/AlGaAs Multiple Quantum Well Waveguides," IEEE J. Quantum Electron. **29**, 2934-2939 (1993).

## 1. Introduction

The theory of the propagation of light within nonlinear waveguides has been explored both analytically and numerically since the early years of nonlinear optics [1-3]. In particular, stability studies have shown that, in a waveguide with an asymetrical nonlinear cladding, light can escape from the waveguide into the cladding region [1-3]. From this, a device called a soliton coupler, in which a second waveguide captures the light emitted by the first, was proposed [4]. This type of highly nonlinear effect requires the local suppression or patterning

#4250 - $15.00 US Received December 15, 1997

of the Kerr nonlinearity in the plane of the device. However, materials in which such effects can be achieved were not available, and the field was abandoned for lack of possible experiments. Recently, it has become possible to create a spatial pattern of the nonlinearity over a multiquantum well (MQW) layer through impurity-free vacancy disordering techniques (IFVD) [5]. In this technique photolithography is used to determine the pattern of the Kerr nonlinear coefficient and can be seen simply as an added step to the fabrication process of integrated optical waveguides in AlGaAs. In this paper we present simulations of a planned experiment using a device based on this technology. As would the first waveguide of the soliton coupler, this device emits light into its cladding region above a given threshold intensity.

## 2. Device characteristics

### *2.1 Basic geometry*

The waveguide is bidimensional in the sense that the light is confined in both axes of the crosssection. First, a guiding layer is grown by molecular beam epitaxy (MBE) over a wafer between two cladding layers. These layers all consist of AlGaAs of varying Al content to provide the proper refractive-index step. The guiding layer consists of a stack of quantum wells. Confinement in the other axis is provided by a $SiO_2$ strip over the top layer. The waveguide is illustrated in Fig. 1.a). The strip is 8 μm wide, the guiding layer is 1 μm thick, and the refractive-index step between the guiding layer and the cladding layers is of the order of 0.1. The effective index method, which will be explained in section 3.1, is used to study more easily (reduction of a two to one dimension problem) the waveguiding in the plane of the wafer. The effective index step in this plane is in the order of $10^{-5}$. The total length of the device is 5 mm. The waveguide mode is represented in Fig. 1.b. It can be indeed deduced by its shape that the confinement in the wafer plane is much weaker than in the vertical axis. It is in this plane that the spatial nonlinear effects will occur, and the strong evanescent field in the cladding region will be put to use. It should be noted that we need the waveguide in order to couple correctly with the device, at low energy.

### *2.2 Patterning the nonlinearity*

We now want to have a waveguide with only one nonlinear cladding (the right-hand region in Fig. 1) and a linear core region. In its as-grown state, of course, the guiding layer is uniform in nonlinearity. The MQW layer exhibits an enhanced nonlinearity compared with its average-composition $Al_xGa_{(1-x)}As$ layer [10]. Disordering the MQW returns the stack to its average composition, and hence suppresses the nonlinearity. In addition, there is an increase in the bandgap of the materials, which also reduces the nonlinearity [9]. By disordering the MQW layer everywhere except in one of the cladding regions, we are left with a waveguide bound by a nonlinear medium on a single side. This resulting device is illustrated in Fig. 1.a. The disordering technique has been demonstrated experimentally with a spatial resolution of less than 1 μm [5], and a reduction of 60% of the nonlinear Kerr coefficient, $n_2$. Our simulations of the propagation within this device were done by means of these real parameters.

Selective disordering using IFVD can be achieved with various techniques [5,6]. The technique used to demonstrate the principle consists of three steps. First, a $SiO_2$ layer is deposited on the wafer and is etched to form a mask. Second, the exposed surface of the wafer is passivated by a hydrogen plasma. Finally, the wafer is thermally treated with a rapid thermal annealer. Upon thermal processing of the wafer, the vacancies associated with the Ga out-diffusion in the regions covered with the $SiO_2$ caps cause intermixing of the MQWs. Therefore only the portion of the MQW layer that is located under the $SiO_2$ mask is disordered, retaining properties close to that of its average composition. The mask used for this device covers the waveguide region and one of the cladding regions. Thus the MQW layer in the cladding region that is not under the mask will remain close to the as-grown condition.

#4250 - $15.00 US Received December 15, 1997

Once the disordering is performed, we can etch away the portion of the $SiO_2$ mask over the linear cladding, keeping only a strip over the waveguide region. This strip provides the confinement effect in the wafer plane.

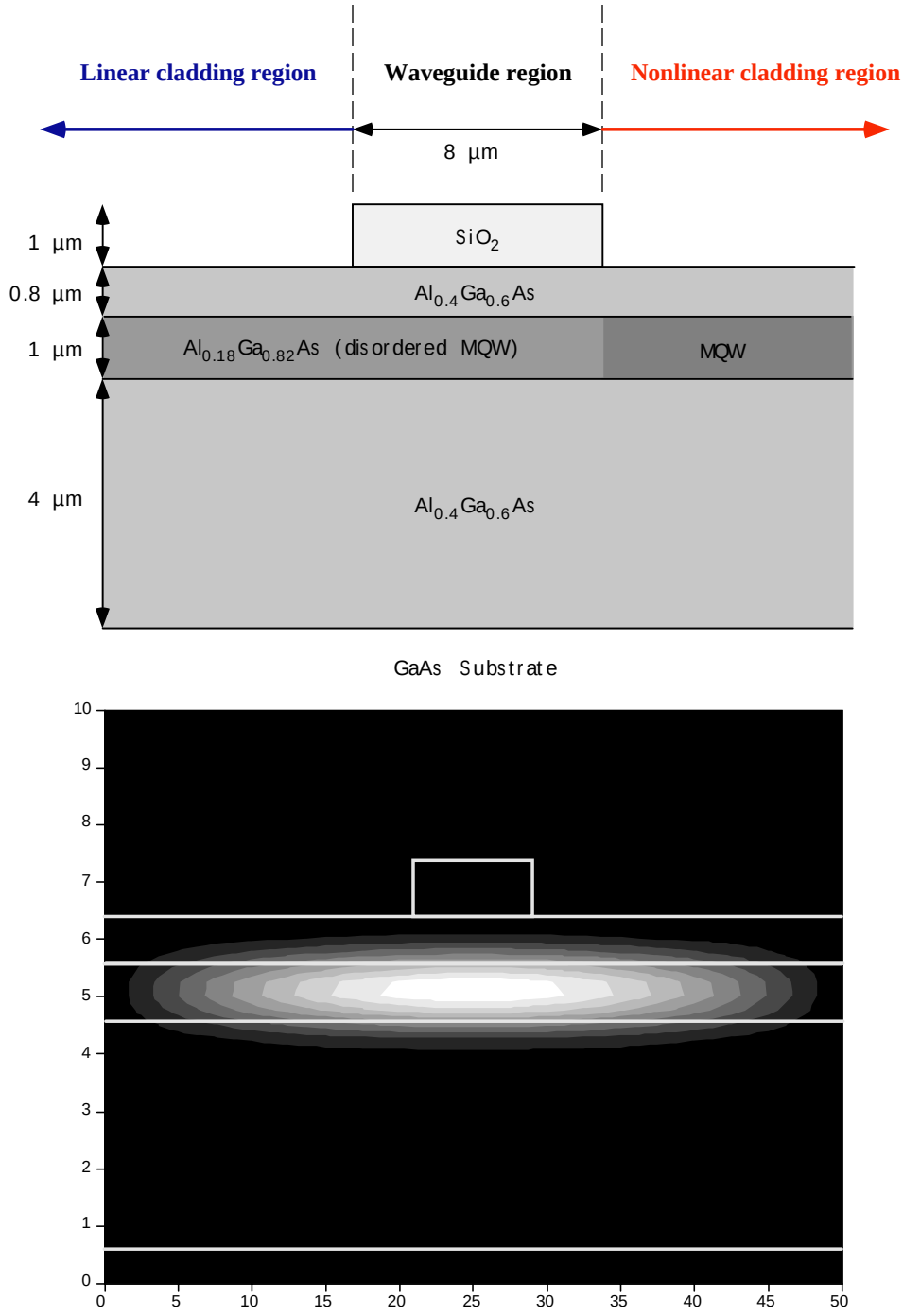


Fig. 1. a) The waveguide structure (top). b) The waveguide mode (bottom). The scales are in µm.

#4250 - $15.00 US
Received December 15, 1997

*2.3 Operation conditions*

The waveguide is designed to be single mode at a wavelength of 1.55 μm. This wavelength is below half the bandgap of the waveguide material so that there will be little or no two-photon absorption.

**3. Simulations**

*3.1 Description*

We have used a one-dimensional spatial beam propagation method (BPM) to simulate the propagation of light within the device. The evolution equation

$$i\frac{dE}{dz} = \frac{1}{2k_o n_{eff}}\frac{d^2E}{dx^2} - \frac{k_o}{n_{eff}}\left[n^2(x) - n_{eff}^2 + 2n_{eff}n_2|E|^2\right]E - \frac{\alpha_0}{2}E \qquad (1)$$

is solved using a fast Fourier transform (FFT) algorithm. We use the effective-index method to reduce the two-dimensional structure into a one-dimensional problem. The effective-index of the mode in the wafer axis is calculated as a function of position along the cross section of the device. This effective index profile is then used in Eq. (1) as $n(x)$. It is perhaps important to remark that although the beam profile is strongly affected in the plane of the wafer, the nonlinear contribution to the mode in the vertical axis can still be treated as a negligible perturbation to the linear mode. In fact, this is quite essential in order to express the nonlinear effective refractive index as it appears in Eq. (1).

The refractive indices used in the simulations are given in refs. 7 and 8. We treat the MQW layer as an average equivalent layer to determine its linear index. The $n_2$ values for the MQW layer and the disordered layer are based on the experimental results given in ref. 5 and agree with theoretical values found in refs. 9 and 10. In a first approximation we neglect all linear and nonlinear absorption. While two- and three-photon absorption are quite negligible, we eventually include the effects of linear and nonlinear absorption to test robustness (see section 6).

We used a Gaussian beam as the input to better simulate the experimental conditions. Since the beam profile does not perfectly match the waveguide mode, the beam shape fluctuates slightly as it propagates.

*3.2 Results*

We show in Fig. 2 the output intensity profile from the waveguide animated as a function of input power. The propagating beam is drawn out of the waveguide region for high input powers. One may also note that a small portion of the beam is emitted in the opposite direction. It is emitted at a steeper angle to conserve momentum. The peak input intensity, required to have most of the power to leave the region below the strip, is of the order of 1.5 GW/cm$^2$ for this device length (5 mm).

#4250 - $15.00 US Received December 15, 1997

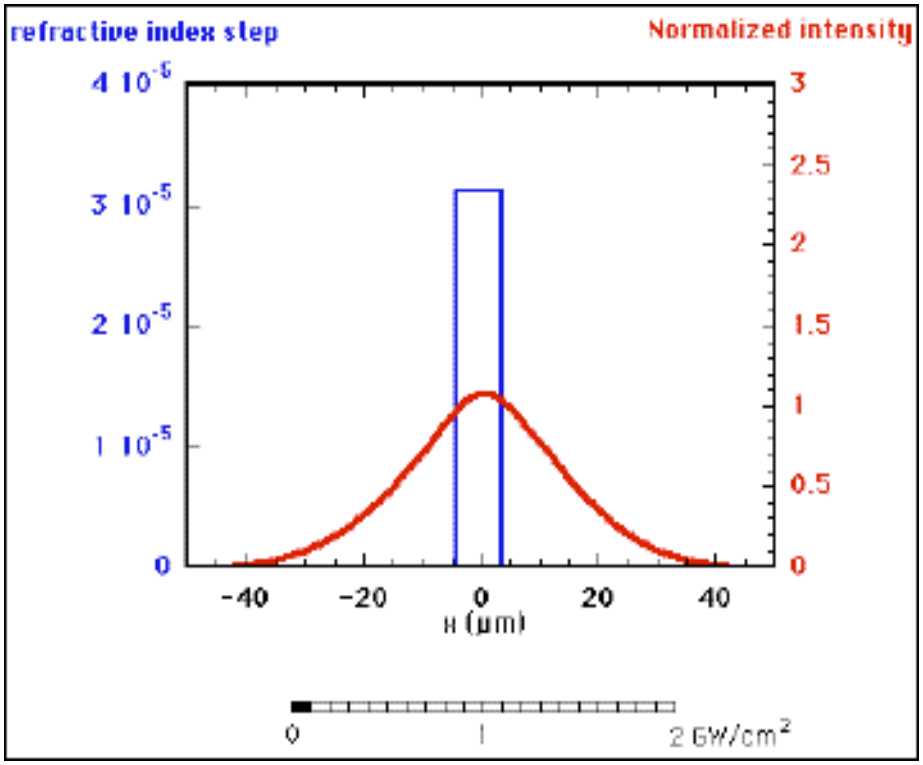


Fig. 2. Movie of the output intensity (in red) from the waveguide (whose index profile is depicted in blue) animated as a function of input power. It can be seen that the peak intensity shifts to the right as the input intensity increases.

## 4. Switching mechanism

The operation of the device is very simple. At low input powers, the propagation within the waveguide can be simulated by a linear model. The light is confined within the waveguide throughout its length, keeping the shape illustrated in Fig. 1.b. The shape actually fluctuates as the Gaussian input beam accomodates itself into the waveguide mode. At higher powers, the intensity dependance of the refractive index becomes noticeable. The highest nonlinear coefficient is, as explained earlier, in one of the cladding regions. The refractive-index step between the core and the cladding is quite small, allowing for a weak confinement resulting in a large mode and hence a sizeable amplitude of the electric field at this interface. The refractive-index step (keep in mind that it is an *effective* index step) at the core-nonlinear cladding interface will decrease as the input power is increased, owing to the difference in nonlinear coefficients between these two regions. At sufficiently high powers, the nonlinear contribution to the refractive features a step that equals and opposes the linear refractive-index step at the interface. The result can be seen in the first frame of Fig. 3. For slightly higher intensities, the index step is reversed and the propagating beam self guides into the cladding region, exiting the waveguide region at an angle. This angle becomes steeper as the input power increases. The minimal switching power is that which makes the index step disappear across the core-nonlinear-cladding interface. We show in Fig. 3 the propagation of the field at

#4250 - $15.00 US
Received December 15, 1997

this minimal switching power. The total refractive index is also shown. It can be seen already in the second frame of this movie that the right-hand index step is reversed. From the subsequent refractive index profile, it is clear that the emission can be interpreted as self guiding, or as a spatial soliton once it has cleared the waveguide region. At the minimum switching power, the corresponding spatial soliton in the nonlinear cladding region has a width of 33 µm.

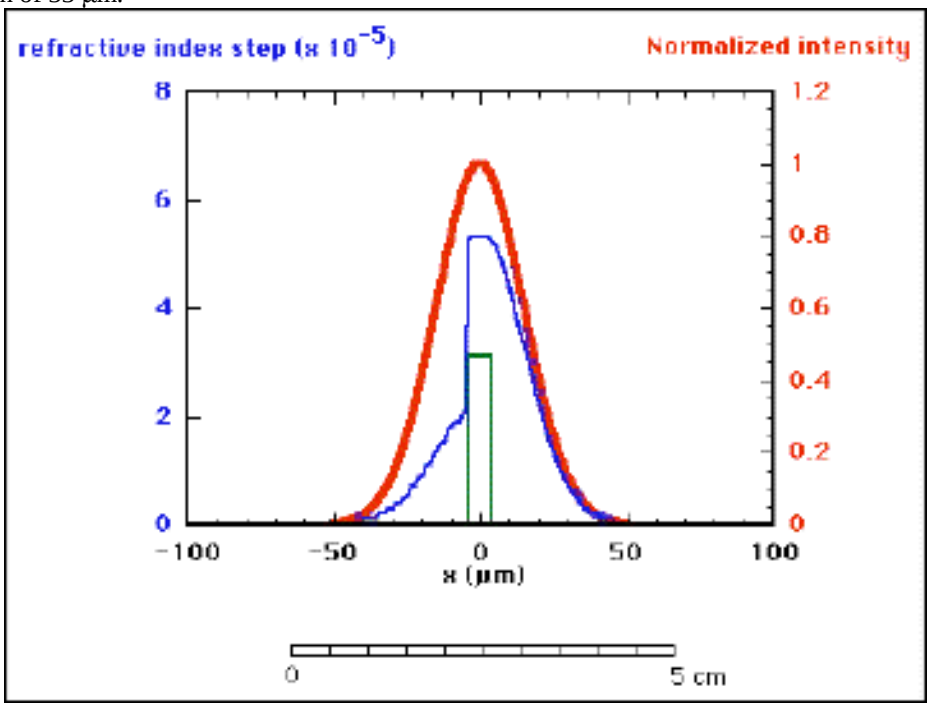


Fig. 3. Movie of intensity (red), linear (green), and nonlinear (blue) refractive, index profiles throughout propagation at the minimum switching power (0.5 GW/cm$^2$ peak). Note that although the propagation length in this figure is 5 cm, the device length is 5 mm.

## 5. Discussion on device length

The switching efficiency can be expressed as the ratio of the spatial displacement of the output beam over the input intensity. The displacement should be large enough to collect both outputs with separate waveguides. Since the displacement is dependent on device length as well on the emission angle, this efficiency could be improved by increasing the device length, and operating at the minimum switching power mentioned in the previous section. It would also improve the switching contrast, i.e., steepen the threshold effect. As seen from Fig. 3, a lossless 5-cm-long device would provide a 30 µm displacement, roughly a beamwidth, at the threshold intensity. However, a longer device would be more sensitive to losses. Since our goal is to demonstrate the experimental feasability, we have concentrated on a shorter 5-mm device.

## 6. Sensitivity to fabrication variations

We have also done some complementary simulations to ensure the device operation is not critical on physical parameters. In this manner we have included linear losses (up to 1 cm$^{-1}$), etch depth (+- 0.1 µm) and etch width (+- 1 µm) variations, and fuzziness (spread over 2µm) of the nonlinear coefficient over the disordered/nondisordered interface. Except for over-

#4250 - $15.00 US
Received December 15, 1997

etching, the device functions properly for any combination of these variations. Indeed, the most critical parameter is the etch depth. The etch determines the effective index step of the waveguide and thus the confinement strength in the wafer plane. The waveguide is also sensitive to asymmetry. If the etch is too deep or too shallow, the waveguide mode can be cut off. The light then drifts towards the highest-index cladding region even at low intensity. In the case of a 0.1 µm overetch, whose high-intensity output is illustrated in curve no. 5 of Fig. 4, the light ends up in the right-hand-side cladding region for both low and high input intensities. The output of the device for a peak input intensity of 1.5 GW/cm$^2$ is shown in Fig. 4 for some variations of waveguide parameters.

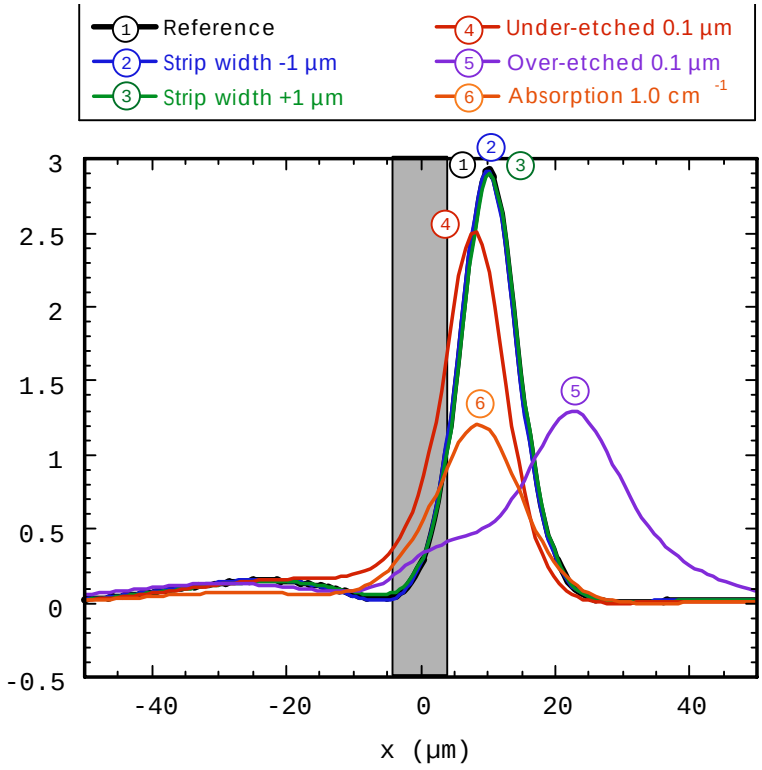


Fig. 4. Output intensity profiles from the device for a peak input intensity of 1.5 GW/cm$^2$ for varying waveguide parameters. Curve no. 1 is the output for the device parameters as specified in section 2. The gray strip delimits the core of the waveguide.

## 7. Conclusion

We have presented an experimentally feasible simulation of an AlGaAs nonlinear device, which can be regarded as either a switch or a thresholding device. The device consists in a linear waveguide with a nonlinear cladding. This is achieved through the selective disordering of a MQW guiding layer. At high enough powers, the index step that forms the waveguide is compensated by the difference in nonlinearity between the two regions, and light self guides into the most nonlinear region, the cladding. It then evolves as a spatial soliton in this region. Simulations demonstrate the expected operation of the device, how the linear refractive-index step gets overwhelmed by the nonlinear index, and shows the tolerance of the device to expected fabrication imperfections. The device is being fabricated and experimental work will start soon.

#4250 - $15.00 US
Received December 15, 1997